International Journal of Engineering & Technology, 7 (4.35) (2018) 728-733

International Journal of Engineering & Technology

Website: www.sciencepubco.com/index.php/IJET

Research paper



Influence of Laminar and Turbulent Flows on Heat Transfer in Liquid-Cooled Plate at Different Fin Arrangements

Fatin Fatihah Abdul Majid[1], Nur Irmawati Om[2], Hasril Hasini[3]*

[1]Department of Mechanical Engineering, College of Engineering, Universiti Tenaga Nasional, Jalan Kajang-UNITEN, 43000 Kajang, Selangor, MALAYSIA
[2]Department of Mechanical & Materials Engineering, Faculty of Engineering & Built Environment, Universiti Kebangsaan Malaysia, 43600 Bangi, Selangor, MALAYSIA
[3]Fluid Dynamics and Disaster Risk Management Research Group, Institute of Sustainability Engineering, Universiti Tenaga Nasional, 43000 Kajang, Selangor, MALAYSIA
**Corresponding author E-mail: hasril@uniten.edu.my*

Abstract

This paper describes CFD investigation of flow and heat transfer in liquid cool plate of a lithium-ion battery. The work aims to compare the cooling performance of an LCP at different fin arrangement for both laminar and turbulence conditions. Prior to the extensive simulation works, the prediction of surface and liquid temperature is first compared made by conducting an experiment using one of the fin arrangement. Good agreement was obtained indicating the ability of the current model to simulate the flow and heat transfer of similar domain at different fin arrangement. The results indicated that the behaviour of the flow and heat transfer is different at laminar and turbulence conditions. The louvered find arrangement showed superior performance in terms of the enhancement of heat transfer. A combination of optimum configurations for fin arrangement and flow condition has enabled excellence overall heat transfer performance of the system.

Keywords: *CFD, Liquid-Cooled Plate (LCP), Battery, Heat Transfer*

1. Introduction

Prius was the first mass-produced electric vehicle by Toyota that was exported globally in 2000. At that time, Toyota used a nickel-metal hybrid battery with conjunction of the research that was done by the Energy Department. But, Honda produced the Insight hybrid in 1999, which was sold in the US only [1]. Tesla Motors started to produce luxurious electric sports car in 2006. Followed by the emergent of plug-in hybrid car by the Volt which has a gasoline engine that supplements its electric drive once the battery is depleted, allowing consumers to drive on electric for most trips and gasoline to extend the vehicle's range. In contrast, the LEAF is an all-electric vehicle, it is only powered by an electric motor. In recent years, the Energy Department's financing in battery research and development has facilitated in cutting electric vehicle battery costs by 50 percent, while concurrently improving the vehicle batteries' performance.

In this modernized era, societies are aware of the harmful effects of internal combustion engines. Internal combustion engines produce more than 30% of the overall global warming emissions. Due to the public's awareness on green mode of transportation, Electric Vehicle (EV) is now rapidly growing [2]. Battery of electric vehicles, which made up around 30% of the automobile industry, made due in specialties where zero-emission requirements, constrained range, and well-defined driving profiles prevailed [3]. It is anticipated that in a long-term, electric and hybrid vehicle will monopolize the main mode of transportation globally.

EV uses packs of Lithium-ion battery. This battery is popular among the other competing technology in the same industry due to several reasons. Li-ion battery is lightweight as it is made up from lithium and carbon. Li-ion battery can hold their charge and only loses about 5% of its charge per month compared to about 25% in nickel-metal hydride (NiMH). Apart from these, lithium ion battery can handle hundreds of cycle of charge-discharge in a system. EV is advancing as the transportation industry is expanding, globally. However, the issue of EV's battery bursting when it reaches the maximum temperature is the main concern of EV manufacturer and also the public. The desired temperature for the battery pack to operate is in between 15℃ - 35℃ [4]. This Li-ion battery in EV is a part of the Battery Thermal Management System (BTMS). BTMS is crucial to ensure the performance and lifespan of an EV. BTMS must be equipped with four essential functions; cooling, heating, insulation and ventilation. BTMS can use a system of either air-cooled, Liquid Cold Plate (LCP) or Phase Change Material (PCM) to maintain the batteries at optimum temperature.

Pesaran and Kim concluded in their work that a mixture of water-ethylene glycol is better than oil for an LCP [5]. Apart from that, Jiang et al. proved that air had the least thermal properties followed by mineral oil then water-ethylene glycol mixture [6]. The study showed that the utilization of liquid cooled yields in better performance than air-cooled system. Meanwhile, in 2015, Rao et al. proposed a parallel configuration of heat sink in order to increase the temperature uniformity in mini channels with 4 cylinders [7]. The result was true but it they also found that the temperature is hard to reduce due to the cylinder's diameter. Sandwiching Li-ion and LCP within the batteries is a method proposed by Somasundaram et al. to analyse the simulation of the LCP to reduce the temperature [8]. The method of sandwiching the LCP results in a better heat transfer performance too.

Copyright © 2018 Authors. This is an open access article distributed under the Creative Commons Attribution License, which permits unrestricted use, distribution, and reproduction in any medium, provided the original work is properly cited.

The interest in LCP is currently expanding. Therefore, more research is in progress of new ways to improve the LCP for a higher efficiency. Other than the type of material being used for the LCP, the arrangement of the fins also will have an impact on the outcome of the heat transfer. Other than this, the conventional straight fins will yield a different result if the fin is changed to other shapes such as straight fin, annular fin, pin fin or an oblique shaped fin. For the purpose of serving the EV, cooling system that uses single-phase liquid such as water-ethylene glycol is the most popular. In order to improve the performance of single-phase liquid-cooled heat ex-changer, micro scale-channels and jet impingement have been widely discussed. However, these technologies make the existing FCV cooling system complicated and expensive. Pin fins arrays mounted on the end wall of the passage play an important role for heat transfer enhancement [9]. The performance of LCP may be varied due to many factors. The performances are correlated from various flow regimes, pin fin arrangements or pin geometry [10].

Although there are very limited research addressing the issues of lithium ion battery for vehicle, according to the U.S. Consumer Products Safety Commission, from 2003 to 2005 more than 300 incidents occurred involving lithium-ion laptop and cell-phone batteries overheating or catching fire. Many of the incidents involved personal injury. The thousands in vehicles multiply this potential problem with lithium-ion batteries. In the case of Tesla Motors' car, for example, almost 7,000 batteries are packed behind the passenger compartment to power the car (to an impressive 60 mph in about four seconds) [11].

The use of LCP in EV battery is monopolizing this sector of the car compared to the use conventional air-cooled battery. A few upgrade and enhancement are being done to improve the battery's performance. The use of straight fins is being switched to oblique-shaped fins to assist disruption of the thermal boundary layer development [9]. Other than that, the types of arrangement of fins in the LCP will also affect the performance to cool the battery [10]. Thus, the main purpose of this study is to investigate the heat transfer and fluid flow characteristics in an LCP channel at different fin arrangement, namely, inline, incline and louvered. The performance of the battery is determined based on surface temperature, cooling liquid temperature, heat transfer coefficient and Nusselt number. In addition, the effect of laminar and turbulent conditions will also be investigated.

2. Description of Simulation Model

2.1. Geometry of LCP

The numerical investigation uses the same geometry of battery that sandwiched the LCP in the middle. Both of the batteries and LCP are made of aluminium and copper respectively, taking these materials properties for the entire simulation. The schematic diagram illustrating the battery and LCP for experiment and simulation is shown in Fig. 1. The battery can be separated into two – top and bottom base. Cooling liquid is allowed to enter the LCP layers through two circular channels located at the left side of the battery system. It will then flows pass an array of fin arrangements before leaving through the second pass, through two circular outlet channels. The size of the batteries and the sandwiched LCP are 390mm × 200mm. The fins are made from a 27° slant at both long edge to create the oblique shape. It is 19mm in length and 2mm width.

Fig. 2(a) shows the inline fin scheme, with a total of 160 fins, arranged in 16 columns and 5 rows, for left and right side of the LCP. The same arrangement and total number of fins are also applied to incline fin arrangement and louvered fin arrangement as shown in Fig. 2(b) and 2(c) respectively. In a straight fin (inline), the arrangement allows a straight flow from the inlet that passes the fins with a small gap of 5mm. For an incline fin arrangement, similar arrangement with inline case applies but the fin is rotated 13° clockwise through the y-axis to allow the slight slant nature to the arrangement. Meanwhile, for louvered fin arrangement, a "V-shape" fin is made, each as a set. A total of 16 columns will have 8 mirrored coupled sets of columns. Rotation of 13° from the y-axis for the right side and mirrored image for the left side. It is important to note that, ethylene glycol flows into the domain from the left side through two channels of inlet and exit on the right side through two outlet channels, with all 4 channels having the same diameter.

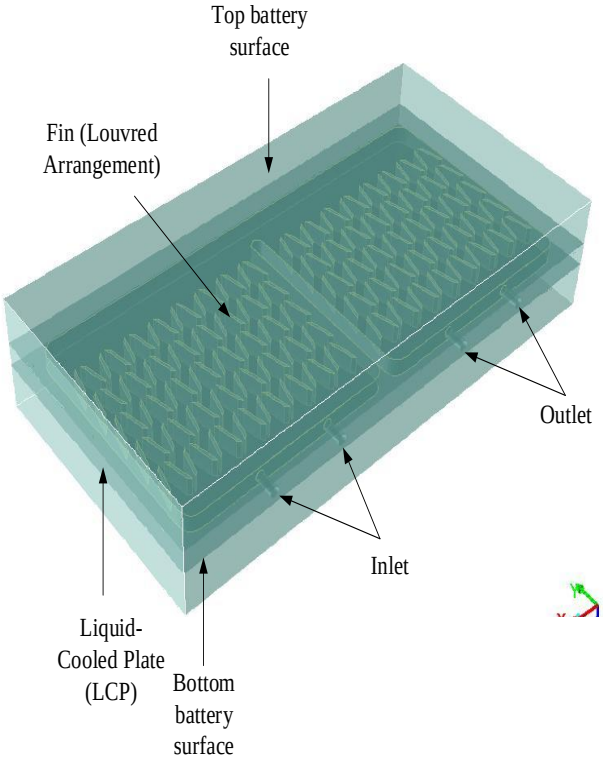


Fig 1: Schematic diagram of battery and LCP arrangement

The flow conditions at the inlet depend on the variation of the velocity set to be manipulated throughout the simulation. In this paper, both laminar and turbulent flow conditions will be studied. Outlet of the coolant flows accordingly to the inlet parameters and also by the nature of the flow in the fluid domain. The fluid flow characteristics are studied throughout the entire area of the LCP.

2.2. Mesh Generation

Mesh generation plays an important role in ensuring good prediction of flow and heat transfer between the fluid and solid domains. Fig. 3 show the general overview of the mesh scheme adopted in this work. Hybrid mesh is used to ensure consistency between very small dimensions that exist the flow domain, particularly in the regions surrounding the fins. Structured mesh is applied on LCP layers while the rest of the flow domain used tetrahedral mesh scheme. The number of mesh is sufficient to ensure that the grid independent solution yields an approximate of 1.1 million cells.

2.3 Governing Equations

In this work, standard governing equations of mass, momentum and energy is adopted, with addition of heat transfer equations. The flow in LCP is assumed to be single-phased. The finite volume method is used to solve the equations. Moreover, the utilisation of second upwind scheme for momentum, continuity, turbulent kinetic energy, turbulent dissipation rate and energy equation, the standard k-ε model and pressure-velocity coupling was found to fit in the implementation. The equations can be expressed as follows:

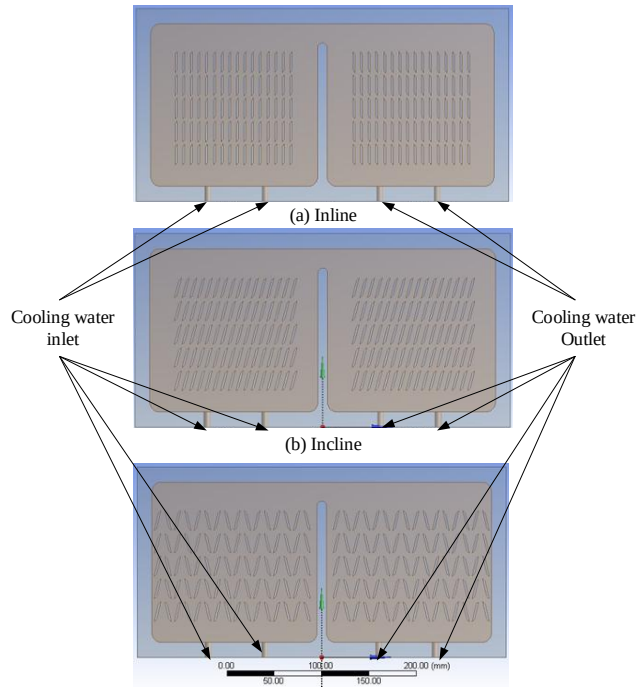


Fig 2: Geometry of battery and CLP at mid cross section for (a) Inline, (b) Incline and (c) Louvered fin arrangement

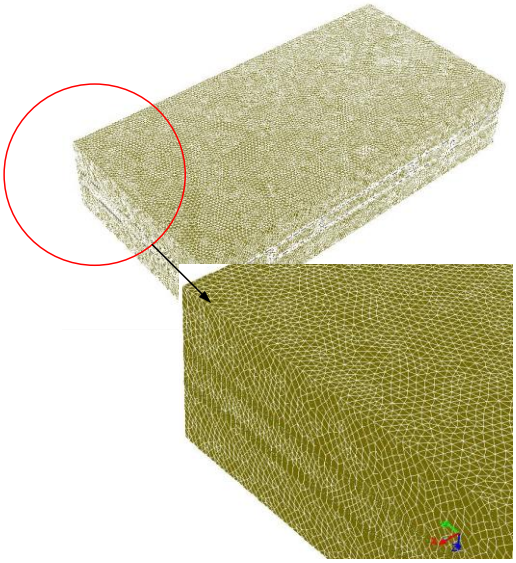


Fig 3: Overall mesh scheme on battery surface

I. Continuity Equation

The mass conservation or continuity equation is as follows:

$$\frac{\partial \rho}{\partial t} = \nabla(\rho u) \tag{1}$$

Where ρ, u and t are density, velocity and time respectively.

II. Momentum Equations

Newton's Second Law states that the rate of increase of momentum of a fluid particle must be equal to the sum of forces on the fluid particle derived the momentum conservation equations. These forces include the body forces and the surface forces. These relations are resolved into x, y and z-axis as shown in equation 2, 3 and 4.

$$\rho\frac{Du}{Dt} = \frac{\partial(-p+\partial\tau_{xx})}{\partial x} + \frac{\partial\tau_{yx}}{\partial y} + \frac{\partial\tau_{zx}}{\partial z} + S \tag{2}$$

$$\rho\frac{Dv}{Dt} = \frac{\partial\tau_{xy}}{\partial x} + \frac{\partial(-p+\partial\tau_{yy})}{\partial y} + \frac{\partial\tau_{zy}}{\partial z} + S \tag{3}$$

$$\rho\frac{Dw}{Dt} = \frac{\partial\tau_{xz}}{\partial x} + \frac{\partial\tau_{yz}}{\partial y} + \frac{\partial(-p+\partial\tau_{zz})}{\partial z} + S \tag{4}$$

III. Energy Equation

The energy equation is casted as follows:

$$\rho\frac{DE}{Dt} = -div(\rho u) + \left(\frac{\partial(u\tau_{xx})}{\partial x} + \frac{\partial(u\tau_{xy})}{\partial y} + \frac{\partial(u\tau_{zx})}{\partial z}\right) + \left(\frac{\partial(u\tau_{xy})}{\partial x} + \frac{\partial(u\tau_{yy})}{\partial y} + \frac{\partial(u\tau_{zy})}{\partial z}\right) + \left(\frac{\partial(u\tau_{xz})}{\partial x} + \frac{\partial(u\tau_{yz})}{\partial y} + \frac{\partial(u\tau_{zz})}{\partial z}\right) + div(k\cdot gradT) + S \tag{5}$$

IV. Heat Transfer Relations

The temperature difference between the LCP resulted from the heating of batteries and the movement of ethylene glycol in the LCP cavity, is convective in nature. The thermal boundary layer will cause heat transfer from the heated battery surface. Other than that, friction between the LCP and ethylene glycol generates velocity boundary. The heat transfer coefficient is defined as:

$$h = \frac{Q}{\Delta T} \tag{6}$$

where h is the convection coefficient or heat transfer coefficient, Q is the heat flux, A is the cross sectional area and ΔT is the temperature difference surface and free stream.

In heat transfer analysis, Nusselt number, Nu is used to define the effectiveness of the heat transfer process. It can be defined as the ratio of the thermal energy convected to the fluid, to the thermal energy conducted within the fluid. Nu = 1 represents a pure conduction of heat transfer. Nu can be expressed as [3]:

$$Nu = \frac{hL}{k} \tag{7}$$

h, L and k are convection coefficient, length and conduction coefficient respectively.

2.4 Boundary Conditions and Model Assumptions

The inlet cooling liquids were set according to laminar and turbulent cases. A few cases were tested starting from Re = 200 to Re = 1000 for laminar cases, while Re = 3000 to Re = 8000 for turbulence cases. For each case, three fin arrangements were tested for the optimum flow and heat transfer capability. In this work, the working fluid is set to be ethylene glycol. Heat from the battery is assumed to originate from the source at top and bottom bases, thus the outer top and bottom surface wall is fixed at 3,846 W/m2. This heat is assumed from the actual heat supplied in the experiment. Conjugate heat transfer is then calculated through the solids and fins be-fore it is convected to cooling liquid that flows in the LCP layers. The temperature of the liquid is estimated to be less than the boiling temperature of the cooling liquid, thus single phase

assumption is taken. The turbulence kinetic energy for turbulent flow case is assumed to follow the k-e model. This assumption is valid as regions of recirculation were found to be minimal for all cases.

3. Result, Analysis and Discussion

In order to ensure the model assumption used in the simulation is accurate, a set of experimental tests are carried out and the result is used and compared with the prediction of surface temperature for the incline case, at laminar condition. In the experiment, the surface temperature is obtained by using temperature probe, attached to a few locations on the surface of the battery. These temperatures were then averaged over the area. The relations between the surface temperature and Reynolds number of the flowing cooling liquid is shown in Fig. 4. Good agreement is obtained for all range of laminar Reynolds number. The surface temperature reduces as the flow of cooling liquid increases. Higher mass of cooling liquid absorbs larger amount of heat generated on the battery surfaces, leaving lower temperature surface. Even though the numerical simulation has slightly over-predicted the surface temperature for all laminar cases, the deviation is minimal and most importantly, the difference is uniform. A correction factor could be introduced to ensure consistency, if needed.

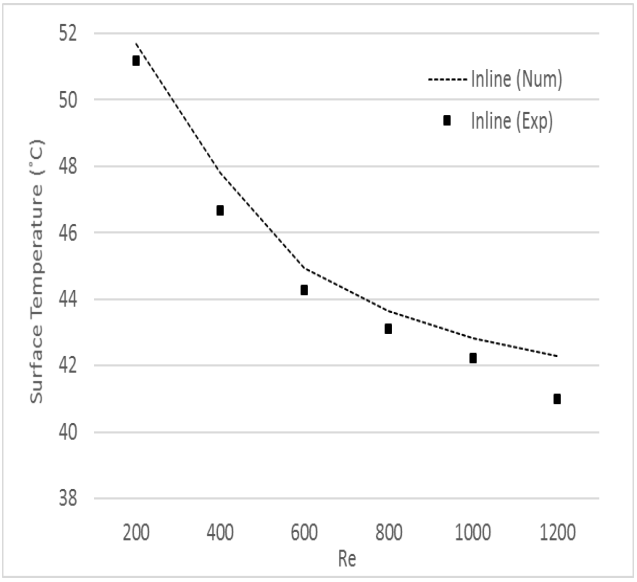


Fig. 4: Comparison of surface temperature between simulation and experimental.

3.1 Battery Surface and Fluid Temperatures

Temperature of battery surface is critical in ensuring safe working condition. Higher battery surface temperature could lead to damage in the materials and thus it is important to understand the cooling of this battery. In this work, three LCP fin arrangements were tested under laminar and turbulent conditions. Even though it is known that turbulence will enhance the dissipation of heat, it is equally important to check whether similar behaviour applies to laminar cases. Fig. 5 shows the surface temperature for laminar cases against the Reynolds number. The general trend shows that the surface temperature reduces when Re increases. Compared between the three fin arrangements, the louvered fin gives the best battery performance with regards to battery surface temperature, followed by the incline and inline fins cases. It can be said that flow mixing effect is better in louvered type arrangement compared to inline and incline. The highest temperature recorded is for inline arrangement at 55.3°C, while the lowest temperature is for louvered at 43.6°C. Louvered arrangements provide better heat transfer thus lowers the battery surface temperature.

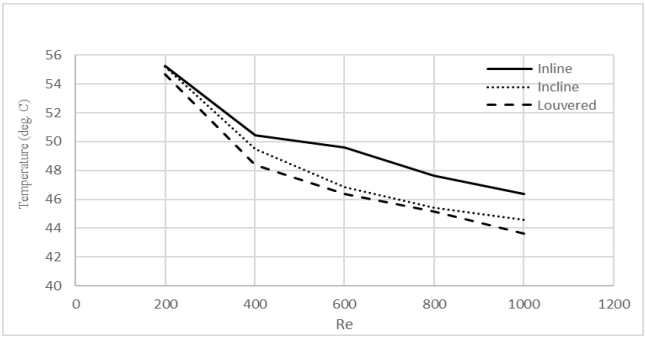


Fig. 5: Battery surface temperature against *Re* for laminar flow

In a turbulent flow, the trend was also found similar – surface temperature reduces when Re increases (as shown in Fig. 6). The louvered fin gives the lowest surface temperature, followed by inline and incline cases. The average surface temperature for turbulent cases was found to be much lower as compared to laminar cases. At turbulence condition, the surface temperature could be further reduced by 10°C.

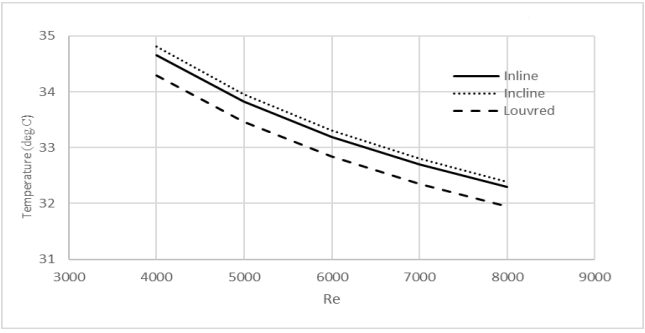


Fig. 6: Battery surface temperature against *Re* for turbulent flow

To gauge the capability of the cooling liquid to absorb heat from battery surface, liquid temperature is also captured for all fin arrangement at both laminar and turbulent conditions. At laminar flow, similar behaviour with surface temperature is noted for the liquid temperature. The liquid temperature reduces as *Re* increases. This can be attributed to the increase of mass flow when *Re* increases. At *Re* less than 700, louvered fin shows the smallest cooling fluid temperature, followed by incline and inline cases. The temperature of cooling liquid could be reduced from 40°C to 32°C using different fin arrangement. It is interesting to note that above *Re* = 700, the trend shows minimum cooling liquid temperature for inline, followed by incline and louvered cases.

In turbulent case, the cooling liquid temperature was found to be much less than the laminar case. Liquid temperature decreases when Re increases. The trend is similar to laminar cases - The average cooling liquid temperature was 27°C (compared to 32-40°C for laminar cases). Comparison between the three fin arrangement, no appreciable difference is noted and all cases shows approximately 27°C liquid temperature. Thus for turbulence case, the fin arrangement does not have significant influence to the cooling liquid temperature. Mixing of fluids happen instantaneously at turbulence condition, enhancing further the heat transfer.

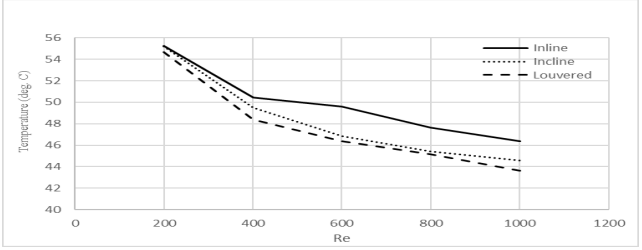


Fig. 7: Fluid temperature against *Re* for laminar flow

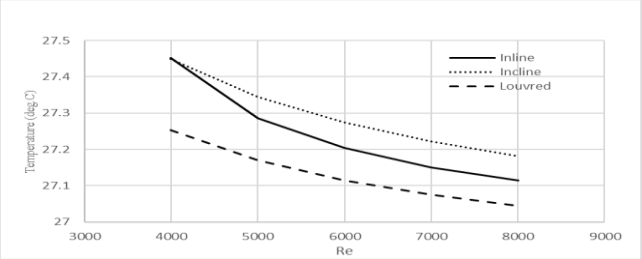


Fig. 8: Fluid temperature against *Re* for turbulent flow

3.2 Heat Transfer Coefficient

The temperature difference between LCP and the moving ethylene glycol in the LCP cavity, causes convection and the thermal boundary layer will cause heat transfer from the heated battery surface. It is also known that friction between the LCP and ethylene glycol generates velocity boundary. Fig. 9 shows the heat transfer coefficient against Reynolds number at laminar conditions. All three fin arrangements were seen to have a steady increase in heat transfer coefficient when the flow speed increases within laminar condition. However, inline and incline arrangements show a sharp drop in heat transfer coefficient at *Re* = 1000. From Equation 6, as the temperature difference increases, heat transfer coefficient decreases. As the battery heats up, and the coolant pumped in the LCP at a high velocity, it shoots up the rows of the fins without lots of boundaries to block the flow movement. The arrangements allow the coolant to pass with very minimal convection. On the other hand, louvered type arrangement tops the graph at every velocity, indicating that the temperature difference between the battery surface and the coolant is small. The coolant is well spread and heat transfer occurs better. The flow mixing effect is better seen at higher *Re* [2].

In turbulent flow, the heat transfer coefficient increases with *Re* as shown in Fig. 10. The magnitude of the heat transfer coefficient is also found to be higher than laminar cases. Comparison between the three fin arrangement, it is clear that the louvered fin gives the highest heat transfer coefficient at both laminar and turbulent conditions. The heat transfer coefficient profiles for turbulent case show linear trend for all cases.

3.3 Nusselt Number

Fig. 11 illustrates the Nusselt number *(Nu)* relations against *Re.* at laminar condition. The trend shows that *Nu* increases as *Re* increases. Higher flow enhances the convection performance, i.e. increase heat transfer. Louvered arrangement shows the highest *Nu* when *Re* increases. When cooling velocity increase, the thermal boundary layer decreases. This is due to the ratio of convection to the fluid and within the fluid is high. The heat from the heating battery is transferred to the coolant efficiently and so does the circulation of heat within the coolant itself. In spite of this, the trend for the inline and incline lines follows the same pattern as the heat transfer coefficient. They experience a sharp drop at *Re* of 1000. When heat is supplied to the LCP, the molecules vibrate faster and heat is supposed to be transferred better too. In these 2 arrangements, the heat convection to the coolant might be better but the heat transfer within the coolant is not. This is due to the high velocity at the inlet.

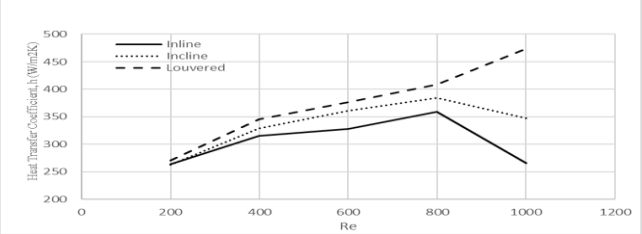


Fig. 9: Heat transfer coefficient against *Re* for laminar flow

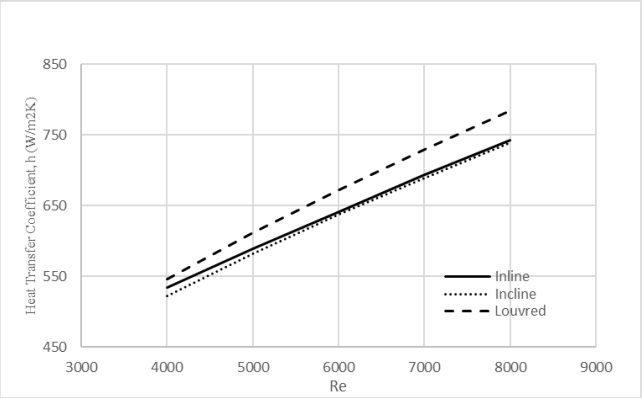


Fig. 10: Heat transfer coefficient against *Re* for turbulent flow

In turbulent cases, similar trend is observed – Increase Nu when Re increases. The overall analysis shows that louvered fin gives the highest Nu, followed by incline and inline respective. The magnitude of Nu for turbulent is far more superior than the laminar cases.

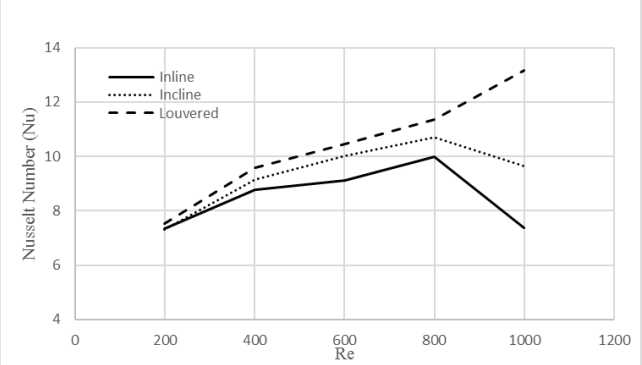


Fig. 11: *Nu* against *Re* for laminar flow

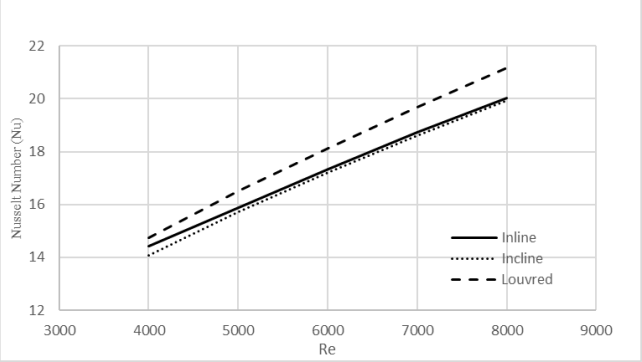


Fig. 12: *Nu* against *Re* for turbulent flow

4. Conclusion

Numerical investigation of LCP battery cooling performance has been successfully carried out to analyse the heat transfers and fluid flow characteristics of different fin arrangements, at different flow conditions. To carry out this analysis, CFD is utilized to simulate the heat transfer and fluid flow inside the LCP and also on the battery itself. In this study, it can be concluded that from all three arrangements namely inline, incline and louvered, louvered type arrangements displays the best heat transfer and fluid flow at both laminar and turbulence conditions. This is better with the increment of the velocity of the fluid inlet. The temperature, heat transfer coefficient, Nu and temperature and velocity contour all points to the fact that louvered will be the best arrangement to cool EV batteries.

Acknowledgement

The authors would also like to acknowledge the financial assistance received from UNITEN Internal Research Grant (UNIIG) that enable the work to be carried out.

References

[1] US Department of Energy. (2014, September) The History of The Electric Car. [Online]. https://energy.gov/articles/history-electric-car
[2] D. Pyke, P. Steenhof S. Brown, "Electric vehicles: The role and importance of standards in an emerging market," Energy Policy, vol. 38, pp. 3797 - 3806, March 2010.
[3] G. Gutmann, "APPLICATIONS – TRANSPORTATION | Electric Vehicle: Batteries," Reference Module in Chemistry, Molecular Sciences and Chemical Engineering, pp. 219 -235, 2009.
[4] National Renewable Energy Laboratory. (2011, September) Electric Vehicle Battery Thermal Issues and Thermal Management Techniques. [Online].
[5] A. A. Pesaran, G. H. Kim, "22nd International Battery, Hybrid abd Fuel Cell Electric Vehicle Conference and Exhibition," , Yokohama, Japan, 2006.
[6] Z. Rao, Y. Li J. Zhao, "Thermal performance of mini-channel liquid cooled cylinder based thermal management for cylindrical lithium-ion power battery," Energy Conversion and Management, vol. 103, pp. 157-165, October 2015.
[7] K. Somasundaram, E. Birgersson, AS Mujumdar, C. Yap W. Tong, "Numerical investigation of water cooling for a lithium-ion bipolar battery pack," International Journal of Thermal Sciences, vol. 94, pp. 259-269, August 2015.
[8] B. Gu, P. Zhao, C. Qian T. Wang, "Numerical investigation of liquid cooling cold plate for power control unit in fuel cell vehicle," Microelectronics Reliability, vol. 55, no. 7, pp. 1077-1088, June 2015.
[9] A. Kosar, C. Mishra, C. J. Kuo, B. Schneider Y Peles, "Forced convective heat transfer across a pin fin micro heat sink," International Journal of Heat and Mass Transfer, vol. 48, no. 17, pp. 3615-3627, August 2005
[10] K. Bullis. (2006, August) Are Lithium-Ion Electric Cars Safe? [Online], https://www.technologyreview.com/s/406201/are-lithium-ion-electric-cars-safe